



UNIVERSITÀ DEGLI STUDI DI NAPOLI FEDERICO II  
SCUOLA POLITECNICA E DELLE SCIENZE DI BASE



**CORSO DI LAUREA  
IN  
INGEGNERIA ELETTRICA**

TESI IN

ELETTROTECNICA

**MODELLAZIONE E SIMULAZIONE DI NANO-OSCILLATORI  
SPINTRONICI COMANDATI IN CORRENTE**

**MODELLING AND SIMULATION OF CURRENT-DRIVEN  
SPINTRONIC NANO-OSCILLATORS**

CANDIDATO:

**DANIELE OLIVIERI**  
MATR. N42000902

RELATORE:

**PROF. MASSIMILIANO D'AQUINO**

ANNO ACCADEMICO 2021/2022



## **RINGRAZIAMENTI**

Ringrazio il Prof. Massimiliano d'Aquino, mio relatore per l'aiuto e il supporto fornитоми nella stesura di questo elaborato.

Ringrazio i miei genitori per avermi consentito d'intraprendere questo percorso e per tutto il sostegno fornитоми in questi anni.

Ringrazio Cristina per avermi sopportato in questi anni e avermi sempre motivato ad andare avanti nonostante le mille difficoltà.

Ringrazio tutti i miei amici e i miei colleghi elettrici che sono stati presenti nella mia vita, con i quali ho condiviso gioie e dolori di questo percorso.



# SINTESI

Lo scopo di questa tesi è di descrivere, analizzare e simulare un nano oscillatore spintronico. Lo sviluppo di questi dispositivi si basa su due principi fisici del magnetismo dei sistemi nanoscopici. Il primo è quello della magnetoresistenza gigante (GMR) scoperta nel 1988 per opera dei Nobel per la Fisica 2007 Albert Fert e Peter Grünberg[1]. Il secondo effetto, noto come Spin-Transfer-Torque (STT) è stato scoperto più recentemente nel 1996 come riportato da J.C. Slonczewski e L. Berger[2, 3].

L'oscillazione della magnetizzazione prodotta dalla corrente continua (DC) che attraversa il dispositivo magnetico si manifesta come oscillazione della resistenza elettrica di quest'ultimo grazie al fenomeno di magnetoresistenza.

Variando l'intensità della corrente continua, è possibile cambiare la frequenza della tensione a microonde prodotta, realizzando nano-oscillatori comandati in corrente. In questo lavoro di tesi si analizza il modello teorico che descrive il comportamento di un nano-oscillatore spintronico che viene poi simulato in MATLAB.

# SUMMARY

The purpose of this thesis is to describe, analyse, and simulate a spintronic nano-oscillator. The development of these devices is based on two physical principles of magnetism in nanoscale systems. The first one is the giant magnetoresistance (GMR) discovered in 1988 by the Nobel Laureates in Physics 2007, Albert Fert and Peter Grünberg[1]. The second effect, known as Spin-Transfer Torque (STT), was discovered more recently in 1996 by J. C. Slonczewski and L. Berger[2, 3].

The oscillation of magnetization induced by a direct current (DC) flowing through the magnetic device results in oscillations of its electrical resistance due to the magnetoresistance phenomenon.

By varying the intensity of the DC, it is possible to change the frequency of the generated microwave voltage, thus achieving current-controlled nano-oscillators.

In this thesis, the theoretical model describing the behaviour of a spintronic nano-oscillator is analysed and then simulated using MATLAB.



# CONTENTS

<b>Introduction</b>	<b>1</b>
<b>1 Mangetoresistance and spintronic devices</b>	<b>3</b>
1.1 Discovery of magnetoresistance . . . . .	3
1.1.1 Giant magnetoresistance . . . . .	3
1.1.2 Tunnel magnetoresistance . . . . .	4
1.2 Devices . . . . .	4
1.2.1 Microwave devices . . . . .	5
1.2.2 Microwave devices capabilities . . . . .	7
<b>2 Physical model</b>	<b>9</b>
2.1 Maxwell's magnetic model . . . . .	9
2.2 Thermodynamics in magnetized media . . . . .	11
2.3 Free energy interactions . . . . .	12
2.3.1 Complete free energy expression . . . . .	14
2.4 First order variation . . . . .	15
2.4.1 Equilibrium configuration . . . . .	16
2.5 Landau-Lifshitz-Gilbert equation . . . . .	17
2.5.1 Normalized equations . . . . .	18
2.6 Uniform field approximation . . . . .	19
2.7 Precessional switching . . . . .	20
2.8 Spin-transfer torque . . . . .	22
<b>3 Simulation analysis</b>	<b>25</b>
3.1 Simulation setup . . . . .	26
3.2 Precessional switching simulation . . . . .	27
3.3 Current induced switching . . . . .	29
3.3.1 Giant magnetoresistance estimation . . . . .	31
3.3.2 RF analysis . . . . .	32
<b>Conclusions</b>	<b>35</b>
<b>Bibliography</b>	<b>38</b>

<b>A Appendix</b>	<b>39</b>
A.1 Spontaneous decrease of free energy . . . . .	39
A.2 Slonczewski equation to MKSA compact model . . . . .	40
A.3 MATLAB scripts and functions . . . . .	42

# INTRODUCTION

Wireless communication has become an increasingly important part of modern life, with a growing number of devices and applications relying on wireless technology. The number of connected IoT (Internet of Things) devices is expected to reach 30.9 billion by 2025, according to a report by Statista. This represents a significant increase from the estimated 13.8 billion IoT devices in use in 2021 [4]. This high demand requires continuous development of new technologies and materials, not only chipset geometrical scaling. One of the promising technologies in this field has been spintronics devices which exploits the spin of an electron instead of its charge. Furthermore, the integration of magnetic spintronics devices with MOSFET circuits, demonstrated by commercial devices such as STT-MRAM, has opened the possibility of Systems-on-Chip (SoC) integrated circuits with both types of components. Commercial STT-MRAMs are now used as a replacement for embedded flash (eFlash) memory or static RAM (SRAM) in embedded cache memories due to advantages such as easy integration with complementary metal oxide semiconductor (CMOS) technology, low energy consumption, fast switching, and superior endurance.

Common wireless communication systems operate in the GHz range, where major markets are IoT (with bands in the 0.3-5.5 GHz range) and public mobile networks (2G-4G; using bands in the 0.7-3 GHz range). For fifth-generation (5G) networks and beyond, very high frequencies (on the order of hundreds of GHz towards THz) will be needed. As a result, the typical components for wireless communication will have to be adapted to new frequency bands and communication protocols. In addition, energy-efficient, compact and low-cost components will have to be developed to address the energy requirements of the IoT. Spintronic devices cover a broad frequency spectrum from direct current (DC) to THz, which could be useful for the on-chip generation and detection of high-frequency signals. The nanoscale size of MTJ nanopillars, combined with the frequency tuning makes the DC-to-RF conversion of interest for implementation in broadband transmitter (Tx)-receiver (Rx) radio links. In addition, for MTJ nanopillars (typical diameters of 50-500 nm) different complementary frequency ranges can be easily achieved by adjusting the device configuration.

Furthermore, charge-spin conversion effects could potentially be used for information processing with Boolean logic, as well as unconventional computing schemes such as neuromorphic and probabilistic computing. [5].



# CHAPTER 1

## MANGETORESISTANCE AND SPINTRONIC DEVICES

### 1.1 Discovery of magnetoresistance

*Magnetoresistance* is the tendency of a certain material to change the value of its electrical resistance with an externally-applied magnetic field. This phenomenon was discovered by Lord Kelvin in 1856, but the effect was very small at about a 5% of resistance variation. He discovered that, in certain magnetic materials such as nickel and cobalt, the resistance increases when the current is in the same direction as the magnetic force and decreases when the current is perpendicular to the magnetic force [6], this phenomenon is actually called *anisotropic magnetoresistance* (AMR). AMR effect has found a wide range of applications, particularly in the field of magnetic sensors.

#### 1.1.1 Giant magnetoresistance

*Giant magnetoresistance* (GMR), a particular spintronic phenomenon, was discovered in 1988 by Albert Fert and Peter Grünberg [7], this is a quantum mechanical phenomenon, which involves the parallel or antiparallel magnetization in ferromagnetic layers, the effect is much more evident than AMR, so this effect is actually utilized in hard disk drives read head, magnetoresistive random-access memory, biosensors and microelectromechanical systems. The Nobel Prize in physics was awarded in 2007 to Albert Fert and Peter Grünberg for the discovery of GMR [1].

The optimal structure of these devices, in terms of sensitivity, is called “spin-valve”: it is composed by two ferromagnetic layers separated by a non-magnetic conductive layer. One layer magnetization is “pinned” by exchange interaction with an adjacent antiferromagnetic layer, whereas the magnetization of the other layer is free to change with an applied external field. The electrical resistance is lower for a parallel alignment or greater for an antiparallel alignment [8].

The spin of electron is responsible for the magnetic field, each electron can be seen as a spinning

charge particle around a loop which causes a magnetic field as it will be discussed in the next section. The electron spin could only have two different states, and each state has a magnetic moment, if the spin of an electron is parallel with the magnetic field, the electron will undergo low *scattering*, so resistance will be low; vice versa if the spin is antiparallel to magnetization, the electron will be subject to more scattering, so the resistance will be higher [1]. That's why using a two layer setup with a fixed magnetization field on the former layer and a variable magnetization on the latter side can make a “valve” like device as shown in figure 1.1.

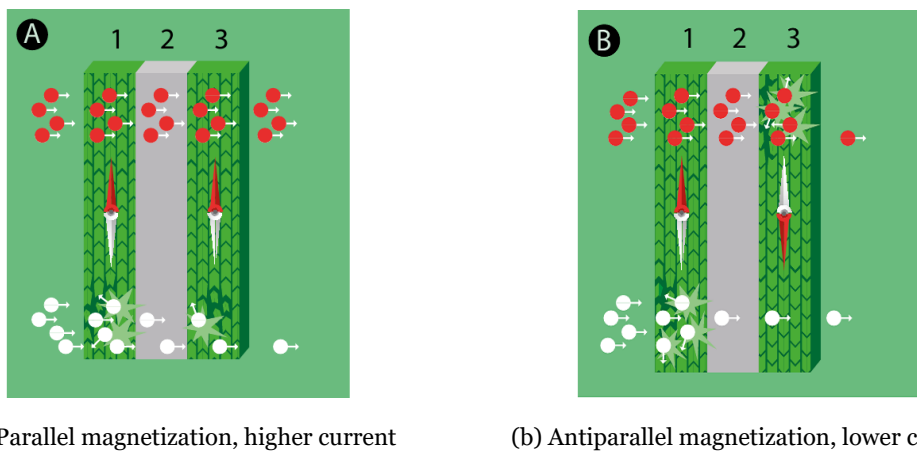


Figure 1.1: Spin-valve device

### 1.1.2 Tunnel magnetoresistance

Another type of magnetoresistance is *tunnel magnetoresistance* (TMR), devices structure is similar to GMR devices but the non-ferromagnetic conductive layer is substituted with an insulating layer (such as magnesium oxide). Electrons have to pass through the device by a tunneling phenomenon. These devices are called *magnetic tunnel junction* (MTJ), the working principle is similar to GMR devices, varying the magnetization of the free layer it is possible to vary the resistance of the device.

## 1.2 Devices

With GMR and MTJ multi layers it is possible to build devices with different purposes, such as magnetic memories, magnetic sensors, radio frequency and microwave devices, and logic and non-Boolean devices, all of these share the same working principle but microwave devices will be specifically analysed in this thesis.

Applying a specific current to the MTJ junction it is possible not only to switch the magnetization state of the free-layer, as it occurs in MRAMs, but also it is possible to “spin” the magnetic field, producing electromagnetic waves as sketched in figure 1.2.

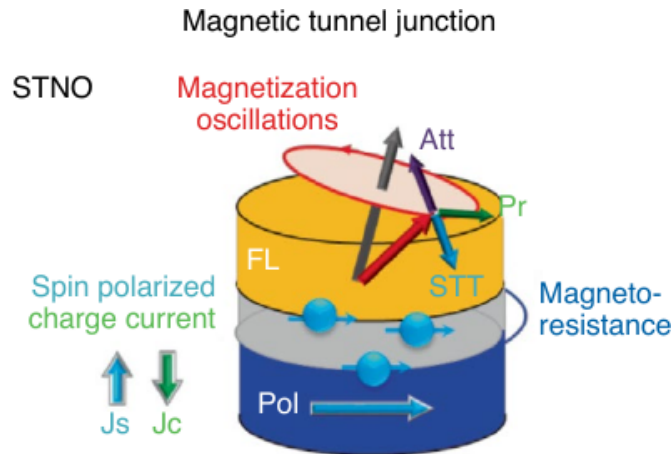


Figure 1.2: Oscillating field in a magnetic tunnel junction

### 1.2.1 Microwave devices

Microwave devices are usually based on two classes: MTJ nanopillars and 2D bilayer structures; MTJ are composed by a multilayer of two ferromagnets separated by a thin insulator layer. The working principle of this class is based on spin-filtering effect, a quantum phenomenon where electrons can “tunnel” across an insulator layer even if they don’t have enough energy according to classical mechanics. The amount of electrons flowing depends on the alignment of the two magnetic fields across the insulating barrier. These fields in a nano-scale device depend mostly on the spin orientation of the electrons in the ferromagnetic layers.

Commonly used materials to build MTJs are ferromagnetic transition metals and their alloys, magnesium oxide ( $MgO$ ) is commonly used as insulator layer. Other materials combinations can be used as shown in figure 1.3 where resistance-area product and magnetoresistance are reported for various materials junctions combinations.

2D bilayer structure have the ability to convert charge currents into spin currents too, or vice versa, through a phenomenon known as spin-orbit coupling. This allows for efficient manipulation of the magnetization dynamics and generation of spin currents in response to applied voltage or current.

GMR spin-valve devices also have the capability to produce a high frequency radiation with a direct current applied, the working principle is different from MTJs, but they have a similar physical model. The next sections will delve further into their investigation.

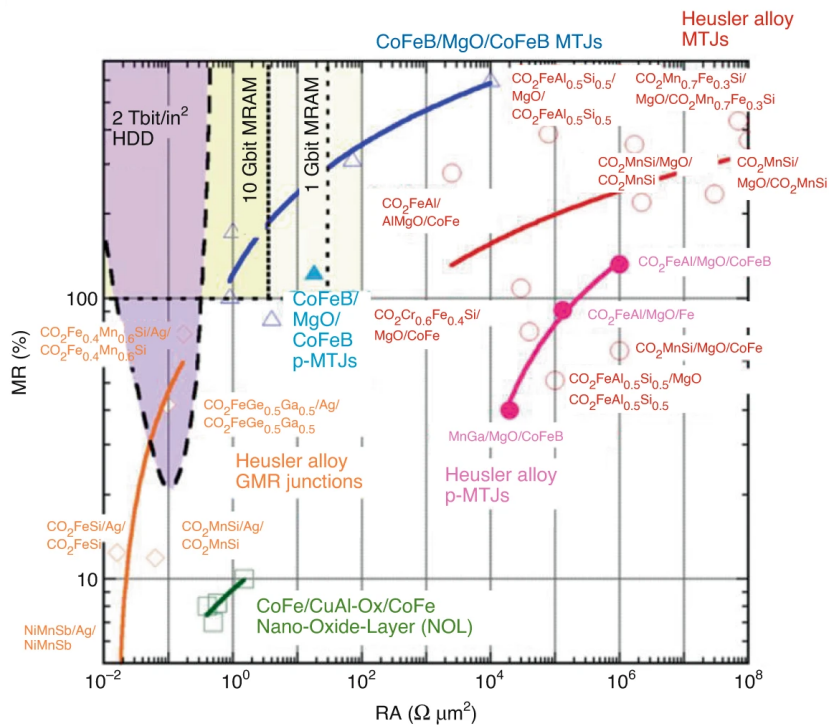


Figure 1.3: Magnetoresistance (MR) and resistance-area product (RA) for various junctions.

## 1.2.2 Microwave devices capabilities

Main functionality of microwave devices is the DC-to-RF conversion, the capability to convert a DC signal to a radio-frequency signal in the band of GHz, this frequency can also be modulated or swept with a proper current signal (fig. 1.4). This functionality is of interest for implementation in broadband transmitter and receiver radio links, amplitude, frequency and phase shift keying protocols can be implemented in a compact way.

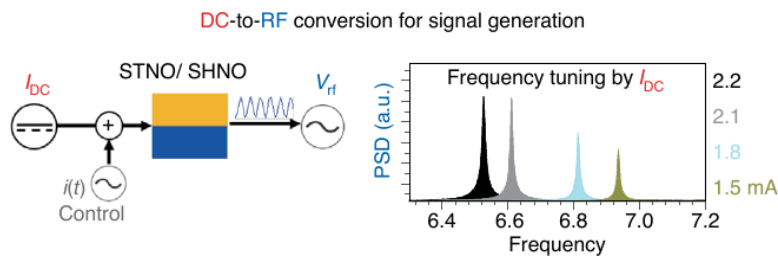


Figure 1.4: Schematic example of a DC-to-RF configuration using an MTJ

The reverse process is possible too with spintronic devices, they can be used as signal detectors with their capability to convert RF radiations to DC signal, they can operate in a low-power passive mode without any power source or in an active-biased mode where an external bias DC current is given in order to get an amplified output voltage.

Another application for these devices is the energy harvesting: a spintronic MTJ could harvest energy from electromagnetic waves available in the environment making self-powered nano-device realization possible [5].



# CHAPTER 2

## PHYSICAL MODEL

Both TMR and GMR devices rely on the capability of the device to change the free layer magnetization state, which is possible due to interaction between the electron spins of the free layer ferromagnet with the spin-polarized current passing through the fixed layer of the device. The Landau-Lifshitz-Gilbert equation knowledge is necessary to properly understand the spin-valve working principle, it will be derived in this chapter from basic magnetism model.

### 2.1 Maxwell's magnetic model

According to Maxwell's equations for electromagnetism, two vectors are used to describe the magnetic field,  $\vec{H}$  and  $\vec{B}$ , the first one is referred to the *magnetic field*, measured in A/m, the second one is referred to as *magnetic induction*, it is measured in T(Tesla) or N/(A · m). In a vacuum they are parallel each other and related by the following:

$$\vec{B} = \mu_0 \vec{H}, \quad (2.1)$$

where  $\mu_0$  is the *vacuum permeability*, equal to  $4\pi \times 10^{-7}$  H/m, anyway a more accurate value was given by CODATA in 2018, it is  $1.256\,637\,062\,12(19) \times 10^{-6}$  H/m [9].

Using the *nabla*( $\nabla$ ) operator it is possible to write the differential magnetic model in a compact way with the *curl* ( $\nabla \times$ ) and *divergence* ( $\nabla \cdot$ ) operations:

$$\nabla \cdot \vec{B} = 0, \quad (2.2a)$$

$$\nabla \times \vec{H} = \vec{J}_{\text{lib}}, \quad (2.2b)$$

$$\vec{B} = \mu_0 (\vec{H} + \vec{M}), \quad (2.2c)$$

$$\vec{H} = \vec{H}_a + \vec{H}_m. \quad (2.2d)$$

The equation 2.2a states that the divergence of the magnetic induction is zero, in other words the field doesn't have any source or sink, the magnetic field is solenoidal. A solenoidal field is a requirement for the magnetic field to be compatible with the Maxwell's equation and the law of conservation of charge [10]. As stated in equation 2.2b the curl of magnetic field is equal to free current density vector  $\vec{J}_{\text{lib}}$ , it is measured in A/m<sup>2</sup>; the magnetic field  $\vec{H}$  is generated by the free current density vector  $\vec{J}_{\text{lib}}$ .

The vector  $\vec{M}$  represents the *magnetization*, measured in A/m like the vector  $\vec{H}$ , it represents how strongly a region of material is magnetized so the magnetic induction  $\vec{B}$  is sum of these two contributes multiplied by  $\mu_0$  (2.2c). The relation between  $\vec{H}$  and  $\vec{M}$  is usually linear in diamagnetic and paramagnetic materials:

$$\vec{M} = \chi \vec{H}, \quad (2.3)$$

where  $\chi$  is the magnetic susceptibility, so the relation between  $\vec{H}$  and  $\vec{B}$  in a material becomes:

$$\vec{B} = \mu \vec{H} = \mu_0(1 + \chi) \vec{H}. \quad (2.4)$$

In ferromagnets these relations are invalid because of magnetic hysteresis. Equation 2.2d presents  $\vec{H}_a$  as the magnetic field in the vacuum,  $\vec{H}_m$  as the magnetic field inside the material. Separating the two  $\vec{H}$  fields it is possible to describe the magnetization inside and outside the material domain called  $\Omega$ . So in  $\Omega_\infty - \Omega$ , which is the external domain, the field  $\vec{H}_a$  is described as follows:

$$\begin{aligned} \nabla \cdot \vec{H}_a &= 0, \\ \nabla \times \vec{H}_a &= \vec{j}_{\text{lb}}. \end{aligned} \quad (2.5)$$

Inside the material domain  $\Omega$  the field  $\vec{H}_m$  is correlated to the magnetization field  $\vec{M}$  with the followings:

$$\begin{aligned} \nabla \cdot \vec{H}_m &= -\nabla \cdot \vec{M}, \\ \nabla \times \vec{H}_m &= 0, \\ \hat{n} \cdot (\vec{H}_{m2} - \vec{H}_{m1}) &= \vec{M} \cdot \hat{n}, \end{aligned} \quad (2.6)$$

where  $\hat{n}$  is the outward normal unit-vector and the last equation of 2.6 is referred to the domain boundary.

Due to small size of domains in exam and slow variations of magnetic fields, it is safe to assume that there are no propagation phenomena and fields are quasi-magnetostatics, so it is possible to ignore time derivatives. To properly analyse the magnetization field behaviour inside a material, a constitutive relation is needed, this is the Landau-Lifshitz-Gilbert equation, a dynamic, non-linear and non-local integral-PDE in the unknown  $\vec{M}(P, t)$ .

## 2.2 Thermodynamics in magnetized media

According to *first thermodynamic law* and *Helmholtz Free Energy* definition:

$$\begin{aligned}\Delta L + \Delta Q &= \Delta U, \\ F &= U - TS,\end{aligned}\tag{2.7}$$

where  $U$  is the system internal energy, function of  $\vec{M}$  and  $S$ ; it is possible to prove that all systems tend to reach minimum energy equilibrium state as discussed in appendix A.1, so the free energy has to decrease to a minimum:

$$\Delta F \leq 0.\tag{2.8}$$

The variable  $\mathcal{M} = \vec{M}dV$  is defined, such that  $\mu_0\mathcal{M}$  is the net magnetic moment present in the volume  $dV$ , so another thermodynamic potential can be explained: the *Gibbs free energy*  $G(\vec{H}_a, T)$ , for constant temperature and external field can be written as:

$$G = \min_{\mathcal{M}} \left[ F - \mu_0 \mathcal{M} \cdot \vec{H}_a \right],\tag{2.9}$$

Similarly to Helmholtz free energy variation, Gibbs free energy variation too is unequal to zero for constant external field and temperature, so the Gibbs free energy has to decrease to a minimum, it depends only on  $\vec{H}_a$  and  $T$  (eq. 2.9); so  $\mathcal{M}$  is a state variable, and it is uniquely determined.

This is not true for ferromagnetic bodies where magnetic domains could also have multiple equilibrium configurations, called *metastable states*, so the generalized Gibbs free energy equation is given to deeper analyse this phenomenon:

$$G(\vec{H}_a, T, \mathcal{M}) = F(\mathcal{M}, T) - \mu_0 \vec{H}_a \cdot \mathcal{M}.\tag{2.10}$$

By differentiating equation 2.10 respect to  $\mathcal{M}$  and imposing a thermodynamic equilibrium it is possible to obtain the following equation assuming  $\mathcal{M}$  as an external constraint:

$$\left[ \frac{\partial G}{\partial \mathcal{M}} \right]_{\vec{H}_a, T} = \left[ \frac{\partial F}{\partial \mathcal{M}} \right]_T - \mu_0 \vec{H}_a = 0,\tag{2.11}$$

otherwise it is not possible to say, with this equation only, which of the possible metastable states the system will reach: Finding a complete expression for  $G$  is necessary to study the phenomenon, it will be done in next sections of this chapter.

## 2.3 Free energy interactions

### Exchange interaction

Exchange interaction is a quantum phenomenon which tends to align neighbour spins. In view of a continuum average analysis, in terms of magnetization vector field, we expect that the exchange interactions tend to produce small uniformly magnetized regions, indeed observed experimentally and called magnetic domains, postulated by Weiss in the early 1900s. Weiss developed a theory postulating, for ferromagnetic materials only, an additional magnetic field  $H_w = N_w M$  called *molecular field*, where  $N_w$  is characteristic of the material.

Weiss ended with following equation [11]:

$$M = M_s \mathcal{L} \left( \frac{\mu_0 m_0 (H_a + N_w M)}{kT} \right), \quad (2.12)$$

where  $M_s$  is the saturation magnetization, and  $\mathcal{L}(\beta)$  is the Langevin function:

$$\mathcal{L}(\beta) = \left( \coth \beta - \frac{1}{\beta} \right), \quad (2.13)$$

it can be developed in Taylor series for small  $\beta$  giving the following linearized equation:

$$M = M_s \left( \frac{\mu_0 m_0 (H_a + N_w M)}{3kT} \right). \quad (2.14)$$

From the 2.14 it is possible to estimate the *Curie* temperature  $T_c$ :

$$T_c = \frac{\mu_0 M_s m_0 N_w}{3k}, \quad (2.15)$$

where  $m_0$  is the permanent magnetic moment of the generic dipole,  $k$  is the Boltzmann constant,  $T$  is the temperature of the medium.

The Weiss theory gives only information about magnitude of magnetization, nothing about direction, so the magnetization vector field can be written as

$$\vec{M}(\vec{r}, t) = M \hat{m}(\vec{r}, t), \quad (2.16)$$

where  $M \simeq M_s$  for temperature  $T < T_c$  as shown in equation 2.12 with  $\hat{m}(\vec{r}, t)$  the unit-vector field.

In order to understand how elementary magnetic moments exchange-interact with one another, the derivation proposed by Landau and Lifshitz, and reported by W.F. Brown Jr.[12] is analysed. An energy term which penalizes magnetization non-uniformities is introduced in the free energy, in the isotropic case this therm is an expansion in even power series of the gradients of magnetization components, stopping the expansion to the first term, the penalization

assumes the following form:

$$f_{ex} = A \left[ (\nabla m_x)^2 + (\nabla m_y)^2 + (\nabla m_z)^2 \right], \quad (2.17)$$

where  $A$  is the exchange constant usually in the order of  $10^{-11} \text{ J m}^{-1}$ . Integrating the 2.17 it is possible to obtain:

$$F_{ex} = \int_{\Omega} A \left[ (\nabla m_x)^2 + (\nabla m_y)^2 + (\nabla m_z)^2 \right] dV. \quad (2.18)$$

## Anisotropy phenomenon

In most experiments one can generally observe that certain energy favoured directions exist for a given material, i.e. certain ferromagnetic materials, in the absence of external field, tend to be magnetized along precise directions, which in literature are referred to as easy directions. To take in account this phenomenon, the magnetization unit-vector needs to be expressed in spherical coordinates with angles  $\theta$  and  $\phi$  such that:

$$\begin{aligned} m_x &= \sin \theta \cos \phi, \\ m_y &= \sin \theta \sin \phi, \\ m_z &= \cos \theta. \end{aligned} \quad (2.19)$$

The anisotropy energy density  $f_{an}(\vec{m})$  is function of the angles  $\theta$  and  $\phi$ , the anisotropy energy will be:

$$F_{an}(\vec{m}) = \int_{\Omega} f_{an}(\vec{m}) dV. \quad (2.20)$$

The most common anisotropy effect and that associated with ferromagnetic materials is the uniaxial anisotropy where only one easy direction exists, supposing that it coincides with the cartesian axis  $z$ . Expanding in series with respect to  $m_z$  (eq. 2.19) and truncating at the second term it is possible to write:

$$f_{an}(\vec{m}) = K_0 + K_1 \sin^2 \theta. \quad (2.21)$$

When  $K_1 > 0$ , the anisotropy energy admits two minima at  $\theta = 0$  and  $\theta = \pi$ , that is when the magnetization lies along the positive or negative  $z$  direction with no preferential orientation, this case is often referred to as easy axis anisotropy. When  $K_1 < 0$  the energy is minimized for  $\theta = \pi/2$ , meaning that any direction in  $xy$  plane corresponds to an easy direction, this case is often referred to as easy plane anisotropy. Integrating the 2.21 on the body, it is possible to obtain the anisotropy free energy:

$$G_{an}(\vec{m}) = \int_{\Omega} K_1 \left[ 1 - (\vec{e}_{an}(\vec{r}) \cdot \vec{m}(\vec{r}))^2 \right] dV, \quad (2.22)$$

where  $\vec{e}_{an}(\vec{r})$  is the easy axis unit-vector in  $\vec{r}$ ,  $K_0$  has been neglected. The character of anisotropy interaction is local: the anisotropy energy related to a generic elementary volume  $dV_{\vec{r}}$  depends only on the magnetization  $\vec{M}(\vec{r})$ .

## Magnetostatic interaction

Recalling the equation 2.2c from the Maxwell model it is possible to express the magnetostatic field as:

$$\vec{H}_m = \frac{\vec{B}_m}{\mu_0} - \vec{M}, \quad (2.23)$$

the energy density of the magnetostatic field is:

$$U_m = \int_{\Omega_\infty} \frac{1}{2} \mu_0 \vec{H}_m \cdot \left( \frac{\vec{B}_m}{\mu_0} - \vec{M} \right) dV, \quad (2.24)$$

where the term  $\vec{H}_m \cdot \vec{B}_m$  is null due to the integral orthogonality of the two fields and  $\vec{M}$  is null outside the body  $\Omega$  so the 2.24 becomes:

$$F_m = - \int_{\Omega} \frac{1}{2} \mu_0 \vec{M} \cdot \vec{H}_m dV. \quad (2.25)$$

Energy in 2.25 can be obtained by computing the work, made against the field  $\vec{H}_m$ , to bring an elementary magnetic moment  $\mu_0 \vec{M} dV$  from infinity to its actual position in the continuous distribution.

## External field interaction

When the external field  $\vec{H}_a$  is considered, it is convenient to introduce the Gibbs free energy functional:

$$G_a = - \int_{\Omega} \mu_0 \vec{M} \cdot \vec{H}_a dV, \quad (2.26)$$

this term, such as the magnetostatic interaction, is a long-range contribution too, it is referred in literature to as *Zeeman energy*.

### 2.3.1 Complete free energy expression

Collecting equations (2.18), (2.22), (2.25), (2.26) it is possible to write the complete expression for the free energy:

$$G(\vec{M}, \vec{H}_a) = \int_{\Omega} \left[ A(\nabla \vec{m})^2 + f_{an} - \frac{1}{2} \mu_0 \vec{M} \cdot \vec{H}_m - \mu_0 \vec{M} \cdot \vec{H}_a \right] dV, \quad (2.27)$$

this equation will be minimized to find the equilibria states,  $\vec{M} = M_s \vec{m}$  so the unknown will be the unit-vector field  $\vec{m}$ .

## 2.4 First order variation

In this section, it is imposed that the first-order variation of  $G$  is zero for each variation  $\delta\vec{m}$  of  $\vec{m}$  so:

$$|\vec{m} + \delta\vec{m}| = 1 \Rightarrow |\vec{M} + \delta\vec{M}| = M_s . \quad (2.28)$$

Each term of eq. 2.27 will be treated separately.

### Exchange variation

By differentiating eq. 2.18 with respect to the magnetization vector field:

$$\delta F_{ex} = - \int_{\Omega} [2\nabla \cdot (A\nabla\vec{m}) \cdot \delta\vec{m}] dV + \iint_{\partial\Omega} \left[ 2A \frac{\partial\vec{m}}{\partial\vec{n}} \cdot \delta\vec{m} \right] dS , \quad (2.29)$$

where the second term comes from the divergence theorem.

### Anisotropy variation

As previous equation, differentiating the eq. 2.22 for an uniaxial anisotropy it is possible to obtain:

$$\delta F_{an} = \int_{\Omega} -2K_1 (\vec{m} \cdot \vec{e}_{an}) \vec{e}_{an} \cdot \delta\vec{m} dV . \quad (2.30)$$

### Magnetostatic energy variation

By differentiating the 2.25:

$$\delta F_m = - \int_{\Omega} \mu_0 M_s \vec{H}_m \cdot \delta\vec{m} dV . \quad (2.31)$$

### Zeeman energy variation

By differentiating the external field energy in equation 2.26:

$$\delta G_a = - \int_{\Omega} \mu_0 M_s \vec{H}_a \cdot \delta\vec{m} dV . \quad (2.32)$$

## 2.4.1 Equilibrium configuration

Putting together equations (2.29), (2.30), (2.31), (2.32), it is possible to obtain the complete variation of free energy for a small magnetic field rotation, in fact the term  $\delta\vec{m}$  can be easily approximated with  $\delta\vec{m} = \vec{m} \times \delta\vec{\theta}$ , the goal is to find minimum energetic configuration, so the energy must vanish, obtaining:

$$\begin{aligned}\delta G = & \int_{\Omega} \vec{m} \times \left[ 2\nabla \cdot (A \nabla \vec{m}) - \frac{\partial f_{an}}{\partial \vec{m}} + \mu_0 M_s \vec{H}_m + \mu_0 M_s \vec{H}_a \right] \cdot \delta\vec{\theta} dV + \\ & + \iint_{\partial\Omega} \left[ 2A \frac{\partial \vec{m}}{\partial \vec{n}} \times \vec{m} \right] \cdot \delta\vec{\theta} dS = 0,\end{aligned}\quad (2.33)$$

where  $\delta\vec{\theta}$  is arbitrary, this lead to two equations:

$$\begin{cases} \vec{m} \times \left[ 2\nabla \cdot (A \nabla \vec{m}) - \frac{\partial f_{an}}{\partial \vec{m}} + \mu_0 M_s \vec{H}_m + \mu_0 M_s \vec{H}_a \right] = 0, \\ \left[ 2A \frac{\partial \vec{m}}{\partial \vec{n}} \times \vec{m} \right]_{\partial\Omega} = 0. \end{cases}\quad (2.34)$$

Second equation of 2.34 is zero only if  $\frac{\partial \vec{m}}{\partial \vec{n}}$  is zero because it is always orthogonal to  $\vec{m}$  which is constant in module. For the first equation of 2.34 the *effective field* can be introduced dividing it by  $\mu_0 M_s$ :

$$\vec{H}_{\text{eff}} = \frac{2}{\mu_0 M_s} \nabla \cdot (A \nabla \vec{m}) - \frac{1}{\mu_0 M_s} \frac{\partial f_{an}}{\partial \vec{m}} + \vec{H}_m + \vec{H}_a, \quad (2.35)$$

the first two terms act on the magnetization as they are two magnetic fields.

The 2.34 becomes:

$$\begin{cases} \mu_0 M_s \vec{m} \times \vec{H}_{\text{eff}} = 0, \\ \left. \frac{\partial \vec{m}}{\partial \vec{n}} \right|_{\partial\Omega} = 0. \end{cases}\quad (2.36)$$

These are called Brown's equations, they allow to find the equilibrium configuration, they are nonlinear because of the dependence of effective field (2.35) on the magnetization field  $\vec{m}$  itself. The first equation implies that the torque exerted by the effective field is null at the equilibrium. The purpose of the next section is to find the dynamic equation to complete the model, this is necessary to describe the evolution of the system.

## 2.5 Landau-Lifshitz-Gilbert equation

A proportionality between the magnetic spin momentum  $\vec{\mu}$  and angular momentum  $\vec{L}$  of an isolated electron is given by quantum mechanics with the next equation:

$$\vec{\mu} = -\gamma \vec{L}, \quad (2.37)$$

where  $\gamma = 2.21 \times 10^5 \text{ mA}^{-1} \text{ s}^{-1}$  is the absolute value of the gyromagnetic ratio [11]. A torque  $\tau$  is applied to the magnetic moment  $\vec{\mu}$  by a magnetic field  $\vec{H}$ , this phenomenon is known as Larmor precession:

$$\tau = \vec{\mu} \times \vec{H}. \quad (2.38)$$

Applying the angular momentum theorem which states that *the change in angular momentum of an object equals the torque applied to it*, it is possible to obtain the following:

$$\frac{d\vec{L}}{dt} = \vec{\mu} \times \vec{H}. \quad (2.39)$$

Combining the 2.39 with 2.37 it is possible to get the expression of the precession of the spin magnetic moment around the magnetic field:

$$\frac{d\vec{\mu}}{dt} = -\gamma \vec{\mu} \times \vec{H}. \quad (2.40)$$

Assuming the field  $\vec{H}$  spatially uniform it is possible to evaluate the precession for each elementary volume and averaging it on the volume it is possible to obtain the continuum gyromagnetic precession model, also called the Landau-Lifshitz equation:

$$\frac{\partial \vec{M}}{\partial t} = -\gamma \vec{M} \times \vec{H}; \quad (2.41)$$

this equation is conservative, so to include the damping effect, the motion of the alignment of the magnetization vector to the  $\vec{H}$  field, Landau and Lifshitz added a term to eq. 2.41 with  $\lambda > 0$  characteristic of the material. The equation 2.41 becomes:

$$\frac{\partial \vec{M}}{\partial t} = -\gamma \vec{M} \times \vec{H} - \frac{\lambda}{M_s} \vec{M} \times (\vec{M} \times \vec{H}). \quad (2.42)$$

In 1955 Gilbert noted that the damping effect could be seen as a “viscous” force, proportional to time derivatives of the field, so the additional torque term is:

$$\frac{\alpha}{M_s} \vec{M} \times \frac{\partial \vec{M}}{\partial t}, \quad (2.43)$$

where  $\alpha$  is the Gilbert damping constant, depending on the material. With this equation too, the magnetization magnitude is preserved so the 2.41 leads to the *Landau-Lifshitz-Gilbert* equation:

$$\frac{\partial \vec{M}}{\partial t} = -\gamma \vec{M} \times \vec{H}_{\text{eff}} + \frac{\alpha}{M_s} \vec{M} \times \frac{\partial \vec{M}}{\partial t}. \quad (2.44)$$

Landau-Lifshitz equation (2.42) can be obtained from Landau-Lifshitz-Gilbert equation (2.44) by multiplying the second one by  $\vec{M}$ , with some vectorial identity it is possible to obtain:

$$\vec{M} \times \frac{\partial \vec{M}}{\partial t} = -\gamma \vec{M} \times (\vec{M} \times \vec{H}_{\text{eff}}) - \alpha M_s \frac{\partial \vec{M}}{\partial t}, \quad (2.45)$$

substituting in 2.44 it is possible to obtain the Landau-Lifshitz equation in the Gilbert form:

$$\frac{\partial \vec{M}}{\partial t} = -\frac{\gamma}{1 + \alpha^2} \vec{M} \times \vec{H}_{\text{eff}} - \frac{\gamma \alpha}{(1 + \alpha^2) M_s} \vec{M} \times (\vec{M} \times \vec{H}_{\text{eff}}), \quad (2.46)$$

where  $\gamma$  is proportional through the Landé factor (approximately equal to 2) to the ratio between the electron mass and charge. Despite both equations are similar, only the LLG equation (2.44) is in agreement with the fact that a very large damping ( $\alpha \rightarrow \infty$ ) should produce a very slow motion, according to physical phenomenon of magnetization dynamics.

### 2.5.1 Normalized equations

In order to investigate which term is prevalent in 2.46 and to easily solve the equation numerically, it is helpful to write the micromagnetic equations in dimensionless units. Free energy equation 2.27 is divided on both sides by  $\mu_0 M_s^2 V_0$  obtaining:

$$\frac{G(\vec{M}, \vec{H}_a)}{\mu_0 M_s^2 V_0} = \int_{\Omega} \left[ \frac{A}{\mu_0 M_s^2} (\nabla \vec{m})^2 + \frac{1}{\mu_0 M_s^2} f_{an} - \frac{1}{2} \vec{m} \cdot \vec{h}_m - \vec{m} \cdot \vec{h}_a \right] dv, \quad (2.47)$$

deriving this equation it is possible to obtain the normalized effective field  $\vec{h}_{\text{eff}} = \vec{H}_{\text{eff}} / M_s$ :

$$\vec{h}_{\text{eff}} = \frac{2}{\mu_0 M_s^2} \nabla \cdot (A \nabla \vec{m}) - \frac{1}{\mu_0 M_s^2} \frac{\partial f_{an}}{\partial \vec{m}} + \vec{h}_m + \vec{h}_a, \quad (2.48)$$

where the term  $l_{ex} = \sqrt{\frac{2A}{\mu_0 M_s^2}}$  is called *exchange length*, it gives an estimation of the characteristic dimension where the exchange interaction is prevalent, usually in the order of 5 ÷ 10 nm, so for the dimension of the bodies considered in this thesis it is appropriate to consider the exchange interaction prevalent on the others forces.

The LLG equation (2.44) can be also calculated in dimensionless form dividing both sides by  $\gamma M_s^2$ :

$$\frac{\partial \vec{m}}{\partial t} = -\vec{m} \times \vec{h}_{\text{eff}} + \alpha \vec{m} \times \frac{\partial \vec{m}}{\partial t}, \quad (2.49)$$

where  $\vec{m} = \frac{\vec{M}}{M_s}$  and  $\vec{h}_{\text{eff}} = \frac{\vec{H}_{\text{eff}}}{M_s}$  and time is measured in units of  $(\gamma M_s^2)^{-1}$ , for  $\mu_0 M_s = 1 \text{ T}$ . The time unit is about 5.7 ps.

## 2.6 Uniform field approximation

In order to numerically solve the magnetization phenomenon with ease, a uniform field approximation is required, this is possible due to the small dimension of the devices in study where, as already cited in section 2.5.1, exchange interaction is prevalent. With this approximation the LLG equation (2.44) needs to be solved in the time and a spatial numerical discretization (such as that obtainable by the finite element method - FEM) is not necessary, so it is assumed that the particle is uniformly magnetized. According to Bertotti G. [13], for an ellipsoidal geometry, the magnetostatic field is expressed by a tensorial relationship with magnetization:

$$\begin{pmatrix} \vec{H}_x \\ \vec{H}_y \\ \vec{H}_z \end{pmatrix} = - \begin{pmatrix} N_x & 0 & 0 \\ 0 & N_y & 0 \\ 0 & 0 & N_z \end{pmatrix} \cdot \begin{pmatrix} \vec{M}_x \\ \vec{M}_y \\ \vec{M}_z \end{pmatrix}, \quad (2.50)$$

where  $N_x$ ,  $N_y$  and  $N_z$  are the *demagnetizing factors* such that  $N_x + N_y + N_z = 1$ . With the uniaxial anisotropy assumption, the corresponding energy term is quadratic, with  $z$  the easy axis, the anisotropy energy term (2.22) becomes:

$$F_{an} = K_1(1 - m_z^2)V_0, \quad (2.51)$$

where  $V_0$  is the volume of the particle. An additional simplifying assumption of rotational symmetry implies that:

$$N_x = N_y = N_\perp, \quad (2.52)$$

under the latter hypothesis, the expression of magnetostatic energy, in dimensionless quantities and neglecting constant terms becomes:

$$g(\vec{m}, \vec{h}_a) = -\frac{1}{2}k_{\text{eff}}m_z^2 - \vec{m} \cdot \vec{h}_a, \quad (2.53)$$

where  $k_{\text{eff}} = N_\perp + \frac{2K_1}{\mu_0 M_s^2} - N_z$ . For symmetry reasons, at the equilibrium, the magnetization lies in the plane defined by the axis  $\vec{e}_z$  and the applied field  $\vec{h}_a$ . If no field is applied, the particle is initially magnetized along the  $z$ -axis, it presents two equilibrium positions for a minimum energy and two positions for a maximum energy. Applying an external field  $\vec{h}_a$ , the free energy still have two minima and two maxima until a critical configuration, increasing  $\vec{h}_a$  up to  $\vec{h}_{SW}$ , where there is only one minimum and one maximum of the free energy. For  $\vec{h}_a < \vec{h}_{SW}$ , the particle field will remain in his initial configuration, then for  $\vec{h}_a \geq \vec{h}_{SW}$  the particle will have only one energy minimum, corresponding to the reversed orientation.

In the general anisotropic case, the effective field will be:

$$\vec{h}_{\text{eff}}(\vec{m}, t) = -\frac{\partial g}{\partial \vec{m}} = -D_x m_x \vec{e}_x - D_y m_y \vec{e}_y - D_z m_z \vec{e}_z + \vec{h}_a(t), \quad (2.54)$$

where  $D$  coefficients take into account shape and crystalline anisotropy, in this case the uniaxial anisotropy is assumed along the  $x$  axis:

$$D_x = N_x - \frac{2K_1}{\mu_0 M_s^2}, \quad D_y = N_y, \quad D_z = N_z. \quad (2.55)$$

Recalling that, when the external applied field is constant, the free energy is a decreasing function of time ( $\alpha > 0$ ), it is possible to conclude that only steady solutions are fixed points, where the number of these points is at least two, and it is even. If the applied field is non-constant, the self-oscillating behaviour cannot be excluded.

## 2.7 Precessional switching

For thin layer structure, magnetization switching can be obtained applying a magnetic field at a certain angle (usually orthogonal) to the initial magnetization field, this causes a torque which pushes the magnetization field out of plane, creating a demagnetizing field perpendicular to the thin plane. The magnetization starts to precess around the demagnetizing field going out of plane, if the external field is switched off when the magnetization is close to its reversed orientation, it will stay reversed. The switching is realized only if the field pulse duration is accurately chosen, if this condition is not met, the magnetization can both switch or not, providing an apparently stochastic phenomenon. Since the film is assumed to be very thin, the demagnetizing factors in the film plane  $N_x$ ,  $N_y$  and  $N_z$  are practically equal to zero and  $-1$ . For a given initial condition, it is necessary a certain field amplitude (critical field for switching). The effective field is so:

$$\vec{h}_{\text{eff}}(\vec{m}) = (Dm_x - h_{ax})\vec{e}_x + h_{ay}\vec{e}_y - m_z\vec{e}_z, \quad (2.56)$$

where  $D = 2K_1/(\mu_0 M_s^2)$ . In order to achieve a switching, the external field must be greater than the critical field here represented in a parametric form [11]:

$$h_{ax} = D \cos \theta \cos^2 \frac{\theta}{2}, \quad h_{ay} = D \sin \theta \sin^2 \frac{\theta}{2}. \quad (2.57)$$

The switching region is represented in figure 2.1, the external field must be inside the shaded region to achieve a complete switching process.

In figure 2.2 a hypothetical magnetization trajectory is shown on the  $(m_x, m_y)$ -plane, trajectory 0 – 1 – 2 can be used to determine the time window for switching off the applied magnetic field.

The relation between time and magnetization is the following [11]:

$$kdt = \frac{du}{\sqrt{1 - (a_x + (p/k) \sin u)^2 - (a_y + p \cos u)^2}}, \quad (2.58)$$

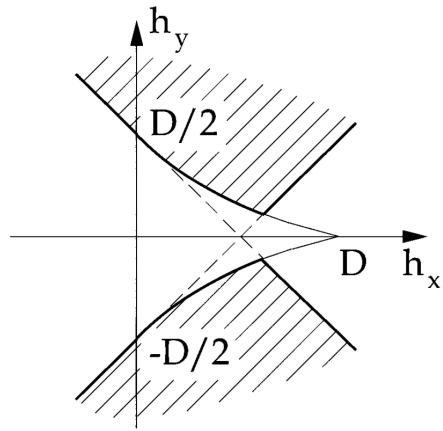


Figure 2.1: Switching region in  $(h_{ax}, h_{ay})$ -plane.

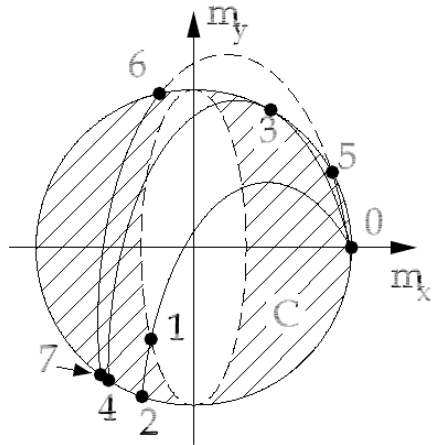


Figure 2.2: Hypothetical magnetic field trajectories on the  $xy$  plane

where  $u \in [0, 2\pi]$  is a parameter,  $k^2 = 1 + D$ ,  $a_x = h_{ax}/(1 + D)$ ,  $a_y = -h_{ay}$  and  $p^2 = h_{ay}^2 + (1 + D)[1 - h_{ax}/(1 + D)]^2$ .

Integrating the 2.58 between points  $u_1$  and  $u_2$  it is possible to find the switch off time window, the optimal time instant is  $T_s = \frac{t_2+t_1}{2}$  when the magnetization is in the closest position with respect to the reversed orientation.

If the external field is perpendicular to the initial magnetization, so it lies along  $y$  axis, the critical field is  $h_c = D/2$ .

## 2.8 Spin-transfer torque

A magnetic effective field exerts a torque on the magnetization vector, this field can be provided by free currents exciting an electromagnet or generated by a *polarized* current. If there are enough electrons with the same spin, or in other words if there is enough current composed of preferentially polarized electrons, they can produce a sufficient torque to allow the switching of the magnetic field.

As described in section 1.1.1 so-called *fixed layer* is used in order to polarize the current, it is mainly made by a ferromagnetic material, magnetized and sufficiently wide. Another layer, thinner, separated by a non-magnetic material is called *free layer*, is initially magnetized too with a planar magnetization as analysed in the previous section.

These stacked layers make a spin-valve device. The spin-polarized electric current injected in the spin-valve can either switch the free layer magnetization or excite a steady magnetic self-oscillation [2]; this is useful in *RF* devices where the aforementioned magnetization oscillation will produce a high frequency electromagnetic radiation with frequencies typically falling in the (microwave) gigahertz range.

Using the next figure 2.3 for reference it is possible to describe and analyse the magnetic dynamics inside a spin-valve device. It is possible to represent with  $\vec{S}_1$  and  $\vec{S}_2$  the macroscopic

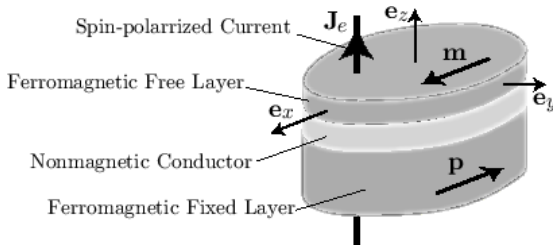


Figure 2.3: Current perpendicular to plane spin-valve device

spin orientation per unit area, of ferromagnetic fixed and free layer, with  $\vec{c}$  the “easy axis” of ferromagnet;  $H_u$  is the anisotropy field constant,  $\alpha$  the Gilbert damping constant,  $J_e$  the current density,  $e$  is the absolute value of the electron charge,  $g$  a scalar function (see equation A.1). Slonczewski derived the following generalized LLG equation with the additional torque term taking into account the effect of spin-polarized currents:

$$\frac{d\vec{S}_2}{dt} = \vec{s}_2 \times \left( \gamma H_u \vec{c} \cdot \vec{S}_2 \vec{c} - \alpha \frac{d\vec{S}_2}{dt} + \frac{J_e g}{e} \vec{s}_1 \times \vec{s}_2 \right). \quad (2.59)$$

With some mathematical steps analysed in appendix A.2 it is possible to obtain the compact

model for spintronics devices in MKSA system:

$$\frac{d\vec{n}}{dt} - \alpha\vec{m} \times \frac{d\vec{m}}{dt} = -\vec{m} \times (\vec{h}_{\text{eff}} + \beta(\vec{m} \times \vec{p})) . \quad (2.60)$$

The effective field can be rewritten as:

$$\vec{\mathcal{H}}_{\text{eff}}(\vec{m}) = \vec{h}_{\text{eff}}(\vec{m}) + \beta\vec{m} \times \vec{p} . \quad (2.61)$$

In this context, the parameter  $\beta = \frac{i}{i_S}$  represents the electric current injected into the spin-valve, normalized with respect to an intrinsic value  $i_S$ . This parameter depends on the type of device under consideration (spin-valve or MTJ) as well as its material and geometric parameters.

The 2.60 becomes:

$$\frac{d\vec{m}}{dt} - \alpha\vec{m} \times \frac{d\vec{m}}{dt} = -\vec{m} \times \vec{\mathcal{H}}_{\text{eff}}(\vec{m}) , \quad (2.62)$$

so the new micromagnetic equilibria condition becomes:

$$\begin{cases} \vec{m} \times \vec{\mathcal{H}}_{\text{eff}}(\vec{m}) = 0 & \Leftrightarrow \vec{\mathcal{H}}_{\text{eff}}(\vec{m}) = \lambda\vec{m} , \\ |\vec{m}| = 1 , \end{cases} \quad (2.63)$$

similar to equations 2.36.



# CHAPTER 3

## SIMULATION ANALYSIS

In order to integrate and simulate the behaviour of the spin-valve in MATLAB environment, the equation 2.60 needs to be rearranged.

The effective field  $\vec{h}_{\text{eff}}$  is given by the following expression:

$$\vec{h}_{\text{eff}} = \vec{h}_a - D_x m_x \vec{e}_x - D_y m_y \vec{e}_y - D_z m_z \vec{e}_z , \quad (3.1)$$

where  $D$  indicates the demagnetizing factor, it takes into account shape and crystalline anisotropy, the free layer analysed and studied in these simulations has  $D_x = -0.1$ ,  $D_y = 0$ ,  $D_z = 1$ , and  $\beta$  is assumed constant (i.e. DC current).

The energy balance of the 2.60 is presented [11]:

$$\frac{dg(\vec{m})}{dt} = -\mathcal{P}(\vec{m}) = -\alpha \left| \frac{d\vec{m}}{dt} \right|^2 + \beta (\vec{m} \times \vec{p}) \cdot \frac{d\vec{m}}{dt} , \quad (3.2)$$

this equation yields the important implication that the spin-transfer torque term can provide energy to the system and counterbalance the Gilbert term dissipation, this will provide a periodic stationary solution of the magnetic field.

The term  $\beta$  should be written as a dimensionless current ratio  $i/i_S$  where  $i_S$  is the intrinsic normalization current, which depends on the type of device and material and geometrical parameters, as mentioned in section 2.8.

$\alpha$  and  $\beta$  are usually both small quantities, the spin-injection can be studied as a perturbation of the case with  $\alpha = 0$  and  $\beta = 0$  so the undamped LLG assumes the form:

$$\frac{d\vec{m}}{dt} = -\vec{m} \times \vec{h}_{\text{eff}} , \quad (3.3)$$

the perturbation is added:

$$\vec{f}_1(\vec{m}) = -\alpha \vec{m} \times (\vec{m} \times \vec{h}_{\text{eff}}) - \beta \vec{m} \times (\vec{m} \times \vec{p}) , \quad (3.4)$$

so the perturbative form of the magnetization dynamics of the free layer is:

$$\frac{d\vec{m}}{dt} = -\vec{m} \times \vec{h}_{\text{eff}} - \alpha \vec{m} \times (\vec{m} \times \vec{h}_{\text{eff}}) - \beta \vec{m} \times (\vec{m} \times \vec{p}) , \quad (3.5)$$

this equation has been numerically integrated in MATLAB using the *ode45* solver, which is the standard MATLAB solver for ordinary differential equations.

## 3.1 Simulation setup

The *MATLAB* script has been organized into *functions* to be versatile and in a way that these functions could be easily called multiple times. All these functions will be reported in appendix at the end of this thesis, but it is important to recall the most important parts in this section. Some constants were easily calculated or imposed at the beginning of the script:

```

mu_0 = 4E-7*pi; % Void permeability [H/m]
Ms = 795E3; % Saturation magnetic field [A/m]
gamma_e = 1.7587E11; % [1/(s*T)] mass to charge ratio
gamma = gamma_e*mu_0; % 1/(s*A/m)
tau = 1/(gamma*Ms); % time unit [s]
K1 = 2E3; % Uniaxial anisotropy constant [J/m^3]
% Intrinsic current density
Jp = 1.6e-19*gamma*Ms^2*3e-9/(2*9.27e-24); % [A/m^2]
% Nanopillar section (130x70x3 nm^3)
S = pi*130/2*70/2*1e-18; % [m^2]
iS_mA = Jp*S/1e-3; % Intrinsic normalization current [mA]
alpha = 2*5E-3; % Damping factor [dimensionless]
Dx = -0.1; Dy = 0; Dz = 1; % Shape and crystalline anisotropy
D = [Dx; Dy; Dz];

```

Listing 3.1: Magnetic constants

The fundamental function which set up the effective field (eq. 3.1) and solves the 3.5 is given:

```

function [t,m] = LLGsolver(D,alpha,p,ha,t_fin,beta,tau)
heff = @ (m,t) ha(t) - diag(D)*m; % Effective field (relative)
LLGprime = @ (t,m) - cross(m,(heff(m,t))) - alpha*cross(m,cross(m,
    heff(m,t))) + beta(t)*cross(m,cross(m,p)); % Perturbative LLG
options = odeset('RelTol',1e-6); % Setting an higher accuracy
% ode45 will integrate the problem
[t,m] = ode45(LLGprime,[0 t_fin],[0.99 sqrt(1-0.99^2) 0],options);
t = t.*tau*10^9; % Time in nanoseconds
end

```

Listing 3.2: Solving the perturbative LLG

## 3.2 Precessional switching simulation

With  $\beta = 0$  and an external applied field the equation 3.5 was solved, the external field lies along the  $y$  axis and is pulsed for a time of 0.1 ns ( $17.57\tau$ ) while the initial magnetization vector  $\vec{m}$  lies along the  $x$  axis, this value was empirically found. The first condition is imposed through the definition of the effective field, the second one is imposed as an initial condition of the differential problem.

```
H = [0; 8E-2; 0]; % Relative field amplitude
% Field pulse duration
hy = @(t) H(2).*((t>(6/tau/10^9))-(t>(6.10/tau/10^9)));
```

Listing 3.3: External field definition

In order to make sure that the solution is independent of the initial conditions, the external field has been applied after waiting 6 ns.

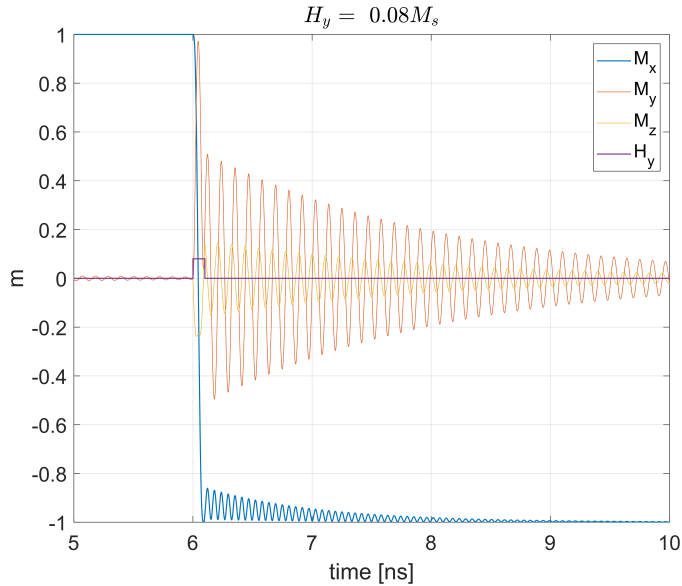


Figure 3.1: Relative magnetization components

In figure 3.1 it is possible to notice how the  $x - axis$  magnetic field component switches from original positive orientation to the reversed one, the external field along  $y - axis$  needs to be applied for a very precise amount of time, otherwise the switching will present a quasi-random behaviour in that the final magnetization can be either the original or the reversed magnetization state for applied fields pulses with very close duration. This could be easily verified with further simulations.

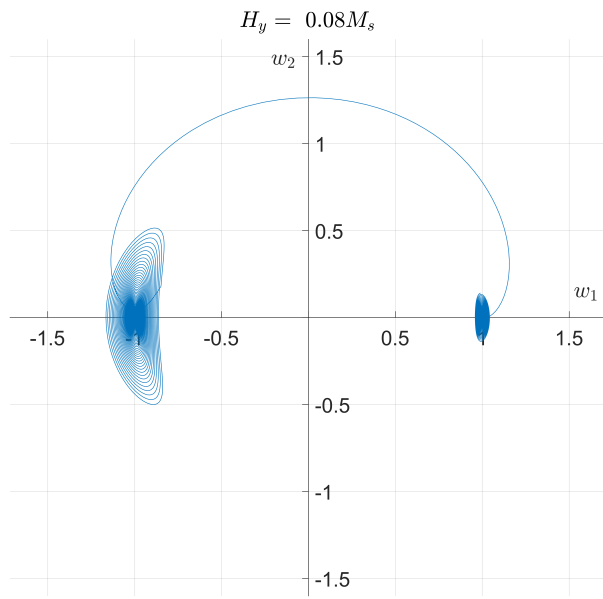


Figure 3.2: Magnetization in stereographic plane

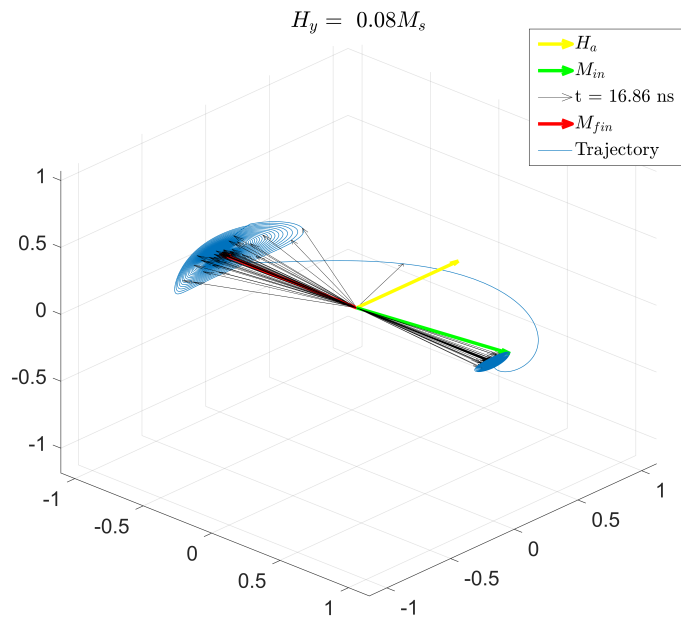


Figure 3.3: Relative magnetization trajectory

A three-dimensional representation is provided in figure 3.3 for a better understanding of the phenomena, the amplitude of the external field vector  $H_a$  is magnified for better visualiza-

tion. From the analysis of the results obtained it is possible to observe that the switching of the magnetic field can be obtained by applying an external field. Nevertheless, the generation of a precise external magnetic field on a nanoscale for such short time is not easy to achieve.

### 3.3 Current induced switching

In order to achieve an easier driving of the device, the spin-transfer effect is utilized, as mentioned in section 2.8. This makes possible to control the device using a specific current and not an external magnetic field, which is also easier to generate and control in a nanoscale system. For this simulation the external field has been set to zero and different values of  $\beta$  have been used. The initial magnetization is parallel with the polarization vector, a positive current will exert a torque on the free layer magnetic field which will tend to reverse its orientation, leading to an increase of the electrical resistance of the device.

```

beta = {@(t) 2*2.90000E-3; % Not sufficient for switching
        @(t) 2*3.33600E-3; % Periodic self-oscillation
        @(t) 2*3.33900E-3}; % Complete switching

px = 1; py = 0; pz = 0; % Polarizing field
p = [px;py;pz];
beta_c1 = -alpha/2*(Dz-Dx+Dy-Dx); % Hopf bifurcation

```

Listing 3.4: Setup for STT simulation

The problem was solved multiple times for each  $\beta$  using a *for* loop, providing the analysis of different behaviours of the spin-valve. The value of  $i_S$  is 25.85 mA, it has been multiplied by  $\beta$  to obtain the effective current value. Anonymous time function of  $\beta$  is defined in order to provide an easy way of eventually set a time-dependent current driving for future simulations where possibly a pulsed signal may drive the device. As it is possible to see, a very small variation of the current can lead to different behaviour. For instance, in figure 3.4 the polarized current is not sufficient to provide a significant torque on the magnetization. Conversely, in figures 3.5 and 3.6, where  $y$  and  $z$  magnetic components have been omitted for better clarity, report the results of simulations for a  $\beta$  value close to the *Hopf bifurcation* that, in the language of dynamical systems theory[11], indicates the critical value corresponding to the appearance of a stable magnetization self-oscillation. For this reason, the behaviours reported in figures 3.5 and 3.6 are different. In figure 3.5 the magnetization oscillates at a certain frequency around the positive  $x$  axis, which is similar to what has been described in section 1.2.2.

Increasing the current amplitude beyond the threshold for *Hopf bifurcation* results in the be-

haviour shown in figure 3.6 where a full switching of free-layer magnetization is achieved, this is useful for the use of the spin-valve as a memory device.

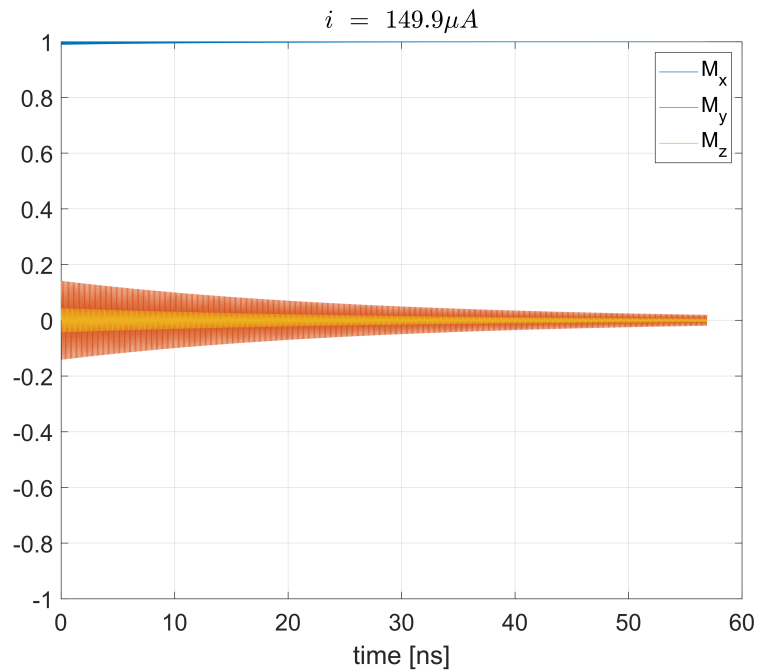


Figure 3.4: No switching

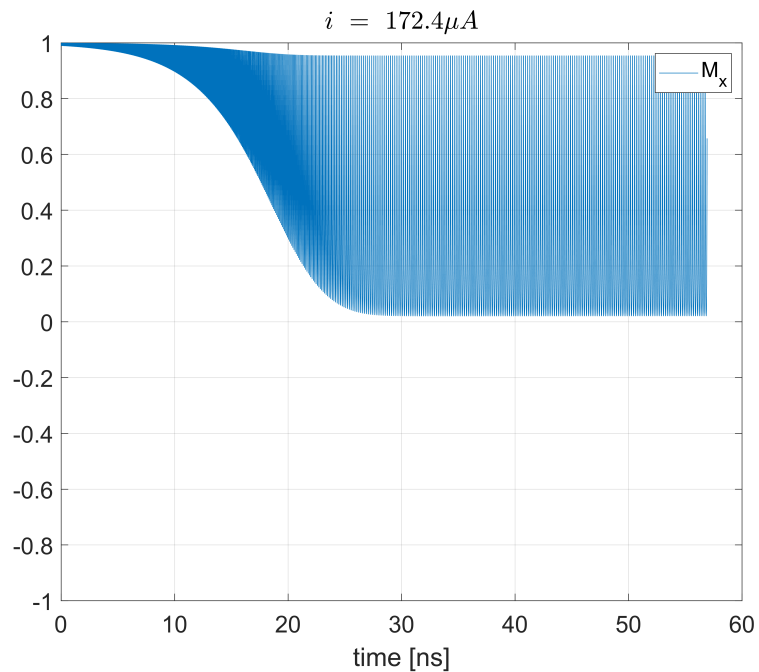


Figure 3.5: Permanent oscillation solution

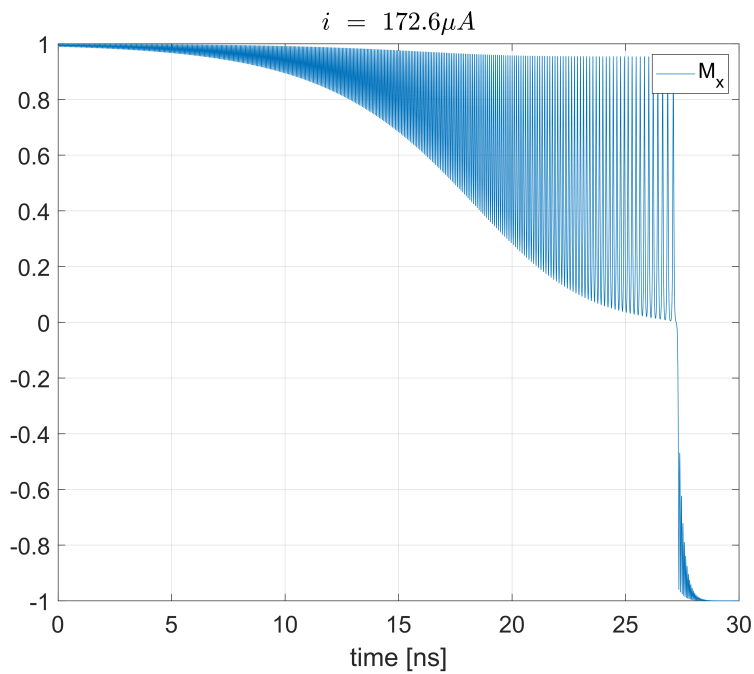


Figure 3.6: Complete switching

### 3.3.1 Giant magnetoresistance estimation

As mentioned in section 1.1.1 the magnetoresistance variation was estimated assuming that it is proportional to the *dot* product between the magnetization vector  $\vec{m}$  and the *pinned* magnetic layer with magnetization vector named  $\vec{p}$ . For illustrative purpose, typical values of resistance for parallel and antiparallel states of free layers magnetizations have been chosen (see Listing 3.5). These in general depend on the device size, material and geometry. Then, the product between resistance and current was plotted in order to analyse the voltage drop across the device, which is the signal eventually read from an oscilloscope.

The case with  $i = 172.4 \mu\text{A}$  is analysed, since this value is close to the *Hopf bifurcation*, for which the oscillation is permanent. Here the magnetoresistance variation is evaluated, then the voltage increase is shown in figure 3.7.

```
R0 = 3e3; % [Ohm]
deltaR = 1e3; % [Ohm]
R = deltaR*dot(m,p'.*ones(length(m),3),2); % m\dot p [Ohm]
plot(t,(R0-R)*i_A); % [Volt]
```

Listing 3.5: Magnetoresistance variation

An increase in resistance is observed due to misalignment of the two magnetic fields caused by

the free layer precession, in agreement with the theoretical model. This increase in resistance is manifested as an increase in voltage across the device, since the applied current is constant in this case.

### 3.3.2 RF analysis

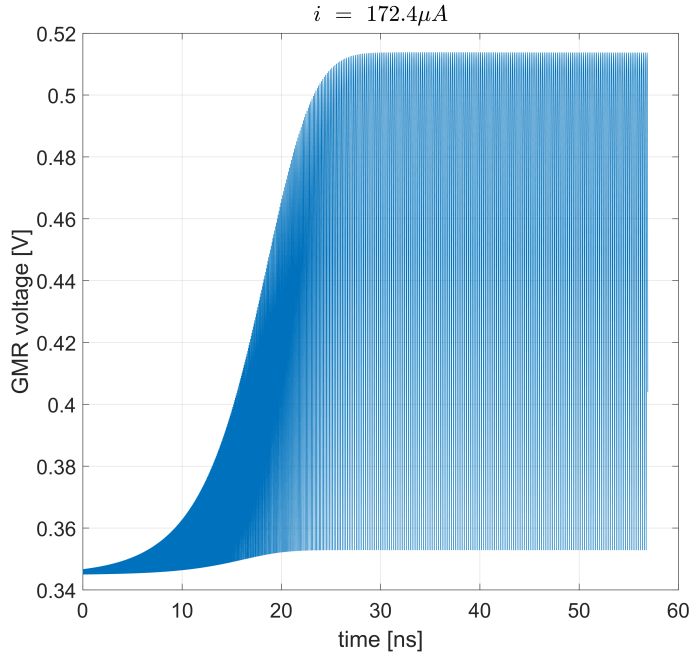


Figure 3.7: Voltage increase

It is also interesting analysing the spectrum of the generated microwave voltage. To this end, methods based on the Fast Fourier Transform (FFT) can be used[14]. In this respect, the voltage FFT is computed and shown in figure 3.8:

```
ind = 20000; % Number of samples
t_sam = linspace(t(end-ind),t(end),ind); % Sampling time
% Interpolating the voltage with more samples
GMR_voltage = interp1(t(end-ind:end),(R0-R(end-ind:end))*i_A,t_sam);
y = fft(GMR_voltage); % FFT compute
freq = (0:length(y)-1)/(t(end)-t(end-ind)); % Frequency vector
% Spectral amplitude plot
semilogy(freq,abs(y/ind),'linewidth',2);
```

Listing 3.6: FFT calculation and plot

We remark that only the last part of the signal (last 28.4 ns) was analysed to wait for the extinction of transient phenomena.

Analysing the figure 3.8 it is possible to notice a DC component in the voltage spectrum, which can be easily filtered, and three principal harmonics, respectively at: 5.287 GHz, 10.61 GHz, and 15.90 GHz. What has been obtained is precisely what was being sought, a high frequency waveform generated with a DC current.

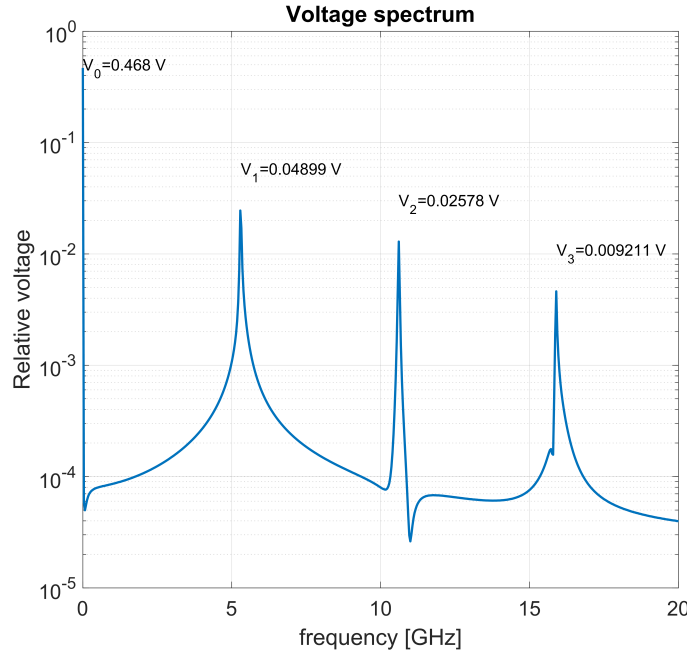


Figure 3.8: Last 28.4 ns voltage spectrum

The second and third harmonics are due to the strong distortion of the voltage waveform shape, caused by the high nonlinearity of the device as can be seen in the figure 3.9. To filter out the DC component, a *bias tee* is inserted between the spin-valve device and a possible antenna as shown in figure 3.10.

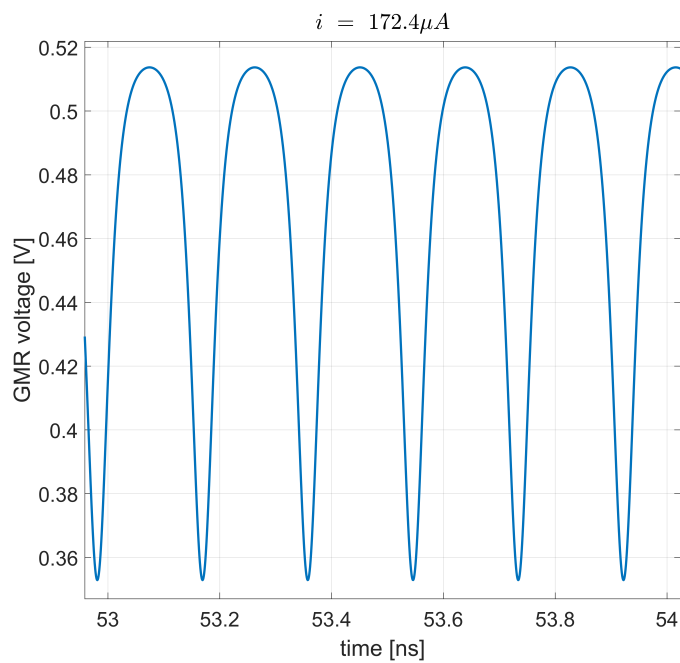


Figure 3.9: Voltage waveform across the device

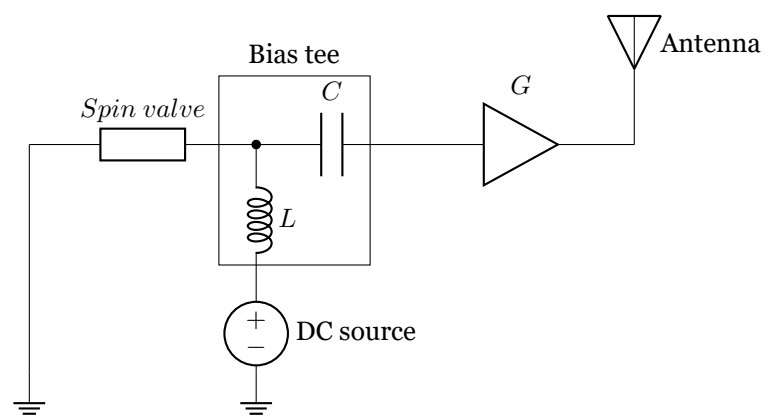


Figure 3.10: Example circuit configuration for RF transmit with spin-valve device

## **CONCLUSIONS**

In conclusion, wireless communication has become an indispensable aspect of our modern society, with the proliferation of IoT devices and the ever-increasing demand for seamless connectivity. Spintronics, with its utilization of electron spin rather than charge, has emerged as a promising technology in the field of wireless communications.

Through this comprehensive analysis of the micromagnetic model and the LLG equation, we have gained valuable insights into the behaviour of spin-valve devices under various conditions. This investigation has contributed to the understanding of the current state-of-the-art and paved the way for future studies in this field.

Moving forward, further investigations are warranted to delve deeper into the intricate phenomena of spin-charge interaction and explore their potential applications. The quest for enhanced performance, reduced power consumption, and improved reliability remains ongoing. Future research endeavours should focus on refining device designs, optimizing material properties, and exploring novel fabrication techniques.

In conclusion, the integration of spintronic devices in wireless communication systems holds great promise for addressing the ever-growing demands of our interconnected world. With continued research and development, we can anticipate the emergence of innovative spintronics based solutions that will revolutionize wireless technologies and reshape our digital landscape.



## REFERENCES

- [1] Albert Fert and Peter Grünberg. *The Nobel Prize in Physics*. 2007. URL: <https://www.nobelprize.org/prizes/physics/2007/press-release/>.
- [2] J.C. Slonczewski. ‘Current-driven excitation of magnetic multilayers’. In: *Journal of Magnetism and Magnetic Materials* 159.1 (1996), pp. L1–L7. ISSN: 0304-8853. DOI: 10.1016/0304-8853(96)00062-5. URL: <https://www.sciencedirect.com/science/article/pii/0304885396000625>.
- [3] L. Berger. ‘Emission of spin waves by a magnetic multilayer traversed by a current’. In: *Phys. Rev. B* 54 (13 Oct. 1996), pp. 9353–9358. DOI: 10.1103/PhysRevB.54.9353. URL: <https://link.aps.org/doi/10.1103/PhysRevB.54.9353>.
- [4] Statista Research Department. ‘Number of Internet of Things (IoT) connected devices worldwide from 2015 to 2025 (in billions)’. In: (Nov. 2016).
- [5] Bernard Dieny et al. ‘Opportunities and challenges for spintronics in the microelectronics industry’. In: *Nature Electronics* 3.8 (2020), pp. 446–459.
- [6] William Thomson. ‘XIX. On the electro-dynamic qualities of metals:—Effects of magnetization on the electric conductivity of nickel and of iron’. In: *Proceedings of the Royal Society of London* 8 (1857), pp. 546–550. DOI: 10.1098/rspl.1856.0144.
- [7] G. Binasch et al. ‘Enhanced magnetoresistance in layered magnetic structures with anti-ferromagnetic interlayer exchange’. In: *Phys. Rev. B* 39 (7 Mar. 1989), pp. 4828–4830. DOI: 10.1103/PhysRevB.39.4828. URL: <https://link.aps.org/doi/10.1103/PhysRevB.39.4828>.
- [8] Candid Reig, Susana Cardoso and Subhas Chandra Mukhopadhyay. *Giant magnetoresistance (GMR) sensors*. Vol. 6. 1. Springer, 2013, pp. 1–301. DOI: <https://doi.org/10.1007/978-3-642-37172-1>.
- [9] Richard H. Parker et al. ‘Measurement of the fine-structure constant as a test of the Standard Model’. In: *Science* 360.6385 (Apr. 2018), pp. 191–195. DOI: 10.1126/science.aap7706. URL: <https://doi.org/10.1126/science.aap7706>.
- [10] John David Jackson. *Classical electrodynamics*. John Wiley & Sons, 2021.
- [11] Massimiliano d’Aquino. ‘Nonlinear magnetization dynamics in thin-films and nanoparticles’. PhD thesis. Università degli Studi di Napoli Federico II, 2004. URL: [http://wpage.unina.it/mdaquino/PhD\\_thesis/main/main.html](http://wpage.unina.it/mdaquino/PhD_thesis/main/main.html).

- [12] W.F. Brown Jr. *Magnetostatic principles in ferromagnetism*. North-Holland Publishing Company, 1962.
- [13] Giorgio Bertotti. *Hysteresis in magnetism: for physicists, materials scientists, and engineers*. Gulf Professional Publishing, 1998.
- [14] E.O. Brigham. *The Fast Fourier Transform and Its Applications*. Prentice-Hall Signal Processing Series: Advanced monographs. Prentice Hall, 1988. ISBN: 9780133075052.  
URL: <https://books.google.it/books?id=XfJQAAAAMAAJ>.

# A

## APPENDIX

### A.1 Spontaneous decrease of free energy

*Proof.* Let a system  $\Omega$  be and  $\Delta L$  and  $\Delta Q$  positive quantities if work or heat is given to the system. If the *work* ( $L$ ) on the system is zero, the *free energy*  $F$  of the system tends to decrease:

$$\Delta L + \Delta Q = \Delta U , \quad \text{first Thermodynamic's Law}$$

$$F = U - TS , \quad \text{Helmholtz Free Energy}$$

$$\Delta F = \Delta U - T\Delta S - S\Delta T ,$$

$$\Delta L + \Delta Q = \Delta F + T\Delta S + S\Delta T ,$$

$$\Delta S = \frac{\Delta Q}{T} + \Delta_i S \geq 0 , \quad \text{second Thermodynamic's Law}$$

$$\Delta Q = T\Delta S - T\Delta_i S ,$$

$$\Delta L + T\Delta S - T\Delta_i S = \Delta F + T\Delta S + S\Delta T ,$$

$$\Delta F = \Delta L - T\Delta_i S - S\Delta T , \quad \text{assuming isothermal process}$$

$$\Delta L = 0 \Rightarrow \Delta F \leq 0 .$$

□

## A.2 Slonczewski equation to MKSA compact model

Slonczewski reported the  $g$  scalar function as follows[2]:

$$g(\vec{s}_1 \cdot \vec{s}_2) = \left[ -4 + (1+P)^3 \frac{(3 + \vec{s}_1 \cdot \vec{s}_2)}{4P^{3/2}} \right]^{-1}, \quad (\text{A.1})$$

where  $P$  is the spin polarizing factor of the incident current which gives the percent amount of electrons that are polarized in the  $\vec{p}$  direction. Using figure 2.3 as reference, it is possible to determine a system of cartesian unit vectors,  $\vec{e}_x, \vec{e}_y, \vec{e}_z$  with the first one equal to vector  $\vec{c}$  in Slonczewski notation and the last one pointing in the direction of fixed layer magnetic field. Changing notations and including the effects of the demagnetizing field  $\vec{H}_m$  and the applied field  $\vec{H}_a$ , the equation 2.59 becomes:

$$\frac{d\vec{S}_2}{dt} = \vec{s}_2 \times \left( \gamma H_{an} (\vec{e}_x \cdot \vec{S}_2) \vec{e}_x - \gamma (\vec{H}_m + \vec{H}_a) \vec{S}_2 - \alpha \frac{d\vec{S}_2}{dt} + \frac{J_e b}{e} \vec{s}_1 \times \vec{s}_2 \right). \quad (\text{A.2})$$

It is now possible to sum the demagnetizing field and the applied field in a unique field  $\vec{H}$  and factoring out the constant vector  $\vec{S}_2$ ; for simplicity it is possible to assume  $\alpha = 0$  and  $J_e = 0$  so:

$$\frac{d\vec{S}_2}{dt} = \vec{S}_2 \times \left( \gamma H_{an} (\vec{e}_x \cdot \vec{s}_2) \vec{e}_x - \gamma (\vec{H}_m + \vec{H}_a) \right).$$

The anisotropy field can be written as follows:

$$\vec{H}_{an} = -H_{an} (\vec{e}_x \cdot \vec{s}_2) \vec{e}_x.$$

By combining the different terms into the effective field, it is possible to obtain the precession equation for the spin vector dynamics:

$$\frac{d\vec{S}_2}{dt} = -\gamma \vec{S}_2 \times (\vec{H}_{an} + \vec{H}_m + \vec{H}_a) = -\gamma \vec{S}_2 \times \vec{H}_{eff}. \quad (\text{A.3})$$

In order to find the relation between  $\vec{S}_2$  and  $\vec{M}$  it is necessary to recall the total magnetic moment  $\vec{\mu}$

$$\vec{\mu} = -\gamma \bar{h} \vec{S}_2 A,$$

where  $A$  is the area of the surface of the device and  $\bar{h}$  the reduced Planck constant; dividing  $\mu$  by the volume  $V$  it is possible to obtain the magnetization vector, where  $d$  is the free layer thickness:

$$\vec{M} = \frac{\vec{\mu}}{V} = \frac{\vec{\mu}}{Ad} = \frac{-\gamma \bar{h} \vec{S}_2 A}{Ad} = \frac{-\gamma \bar{h} \vec{S}_2}{d} = \frac{-g_e \mu_B}{d} \vec{S}_2,$$

where  $g_e$  is the Landé factor for electrons and  $\mu_B$  is the Bohr magneton, so  $\gamma = g_e \mu_B / \bar{h}$ .

Dividing both terms of equation A.2 by  $-g_e\mu_B/d$  and considering  $M_s$  as the saturation magnetization, so  $\vec{m}$  is the unit vector along  $\vec{M}$ , it is possible to obtain the following equations

$$\begin{aligned} \frac{d\vec{M}}{dt} &= -\vec{m} \times \left( \gamma H_{an} (\vec{e}_x \cdot \vec{M}) \vec{e}_x + \gamma \vec{H} M_s - \alpha \frac{d\vec{M}}{dt} + \frac{g_e \mu_B J_e b}{ed} \vec{s}_1 \times \vec{m} \right), \\ \frac{d\vec{m}}{dt} - \alpha \vec{m} \times \frac{d\vec{m}}{dt} &= -\vec{m} \times \left( \gamma H_{an} (\vec{e}_x \cdot \vec{m}) \vec{e}_x + \gamma \vec{H} + \frac{g_e \mu_B J_e b}{ed M_s} \vec{s}_1 \times \vec{m} \right) \text{ dividing by } M_s, \\ \frac{d\vec{m}}{dt} - \alpha \vec{m} \times \frac{d\vec{m}}{dt} &= -\gamma M_s \vec{m} \times \left( k_{an} (\vec{e}_x \cdot \vec{m}) \vec{e}_x + \vec{h} + \frac{1}{\gamma M_s ed M_s} g_e \mu_B J_e b \vec{s}_1 \times \vec{m} \right) \text{ isolating } \gamma M_s. \end{aligned}$$

In the last equation it is possible to find some normalizations  $k_{an} = \frac{H_{an}}{M_s}$  and  $\vec{h} = \frac{\vec{H}_m + \vec{H}_a}{M_s} = \vec{h}_m + \vec{h}_a$ .

It is also possible to define a constant which has the dimension of a current density:

$$J_p = \gamma M_s \frac{e M_s d}{g_e \mu_B}.$$

The last equation of the previous group becomes:

$$\frac{d\vec{m}}{dt} - \alpha \vec{m} \times \frac{d\vec{m}}{dt} = -\gamma M_s \vec{m} \times \left( k_{an} (\vec{e}_x \cdot \vec{m}) \vec{e}_x + \vec{h} + \frac{J_e}{J_p} b \vec{m} \times \vec{p} \right), \quad (\text{A.4})$$

where  $b$  is the scalar function in the new notations:

$$b = b(\vec{m}) = \left[ -4 + (1+P)^3 \frac{(3 + \vec{m} \cdot \vec{p})}{4P^{3/2}} \right]^{-1}.$$

By using the above definitions it is possible to obtain the equation 2.60:

$$\vec{h}_{eff} = k_{an} (\vec{e}_x \cdot \vec{m}) \vec{e}_x + \vec{h}_m + \vec{h}_a, \quad \beta = \beta(\vec{m}) = \frac{J_e}{J_p} b(\vec{m}).$$

## A.3 MATLAB scripts and functions

```
%% Slonczewsky

close all; clear; clc;

mu_0 = 4E-7*pi; % Void permeability [H/m]
Ms = 795E3; % Saturation magnetic field [A/m]
gamma_e = 1.7587E11; % [1/(s*T)] mass to charge ratio
gamma = gamma_e*mu_0; % 1/(s*A/m)
tau = 1/(gamma*Ms); % time unit [s]
K1 = 2E3; % Uniaxial anisotropy constant [J/m^3]
% Intrinsic current density
Jp = 1.6e-19*gamma*Ms^2*3e-9/(2*9.27e-24); % [A/m^2]
% Nanopillar section (130x70x3 nm^3)
S = pi*130/2*70/2*1e-18; % [m^2]
iS_mA = Jp*S/1e-3; % Intrinsic normalization current [mA]
t_fin = {1.0E4; 1E4; 1E4}; % Simulation time
beta = {@(t) 2*2.90000E -3; % Not sufficient for switching
        @(t) 2*3.33600E -3; % Periodic self - oscillation
        @(t) 2*3.33900E -3}; % Complete switching
alpha = 2*5E-3; % Damping
Dx=-0.1; Dy=0; Dz = 1;
D = [Dx;Dy;Dz];
beta_c1=-alpha/2*(Dz-Dx+Dy-Dx); % Hopf bifurcation
px = 1; py=0; pz=0;
p = [px;py;pz];
H = [0;0;0]; % External null field
ha = @(t) H;
hy = @(t) 0;
for i = 1:3
    [t,m] = LLGsolver(D,alpha,p,ha,t_fin{i},beta{i},tau); % LLG
    solve
    titlename = strcat("$i\ = \ ",num2str(iS_mA*beta{i}(0)/1e-3,4)," 
    \mu A$");
    plot_components(m,t,hy,tau,titlename); % Plot magnetization
    components
```

```

plot_trajectory(m,t,p,titlename); % Plot magnetization vector 3D
plot_xy(m,Dz,titlename); % Plot componenti nel piano xy e nel
                           piano stereografico
plot_gmr(m,t,p,tau,iS_mA*beta{i}(0)*1e-3,titlename);
end

%% Precessional switching
%close all;
clear; clc;
t_fin = 3E3;
K1 = 2E3; % J/m^3
mu_0 = 4E-7*pi; % H/m
Ms = 795E3; % A/m
Dd = K1/(mu_0*Ms^2);
gamma_e = 1.7587E11; %1 /(s*T)
gamma = gamma_e*mu_0; % 1/(s*m/A)
tau = 1/(gamma*Ms); % s
beta = {@(t) 0}; % No current
alpha = 5E-3; % Damping
Dx=-0.1; Dy=0; Dz = 1;
D = [Dx;Dy;Dz];
px = 0; py=0; pz=0;
p = [px;py;pz];
H = [0;8E-2;0]; % External field magnitude
% External field duration
hy = @(t) H(2).*((t>(6/tau/10^9))-(t>(6.10/tau/10^9)));
ha = @(t) [0;hy(t);0];
% Solving
[t,m] = LLGsolver(D,alpha,p,ha,t_fin,beta{1},tau);
titlename = strcat("$H_y = \ ",num2str(H(2),3)," M_s$");
plot_components(m,t,hy,tau,titlename);
xlim([5 10]);
plot_trajectory(m,t,H,titlename);
plot_xy(m,Dz,titlename);

```

Listing A.1: spin\_RF.m Main file

```

function [t,m] = LLGsolver(D,alpha,p,ha,t_fin,beta,tau)
heff = @(m,t) ha(t) - diag(D)*m; % Effective field (relative)
% Perturbative LLG
LLGprime = @(t,m) - cross(m,(heff(m,t))) - alpha*cross(m,cross(m,
    heff(m,t))) + beta(t)*cross(m,cross(m,p));
options = odeset('RelTol',1e-6); % Setting an higher accuracy
% ode45 will integrate the problem
[t,m] = ode45(LLGprime,[0 t_fin],[0.99 sqrt(1-0.99^2) 0],options);
t = t.*tau; % Time in seconds
t = t*10^9; % Time in nanoseconds
end

```

Listing A.2: LLGsolver.m Solver function

```

function [] = plot_components(m,t,hy,tau,titlename)
f = figure();
f.Position = [70 250 900 700]; %Window size
plot(t,m(:,1)); hold on;
set(gca,'FontSize',18);
title(titlename,"Interpreter","latex");
% Add the external field
%plot(t,hy(t/tau/10^9));
grid on;
% Add the eventual external field in legend
%legend("M_x","M_y","M_z","H_y");
legend("M_x","M_y","M_z");
legend("M_x");
xlabel('time [ns]');
ylim([-1 1]);
end

```

Listing A.3: plot\_components.m Plot the field components

```

function [] = plot_trajectory(m,t,H,titlename)
d = 100; % Exclude some vectors from printing
new_length = length(t);
axlim = 1.5;
f = figure(); grid on; hold on; axis(axlim*[-1 1 -1 1 -1 1]);
title(titlename,"Interpreter","latex");
f.Position = [70 150 900 800];
set(gca,"FontSize",18);
view([1 -1 0.6]); %camera position in x,y,z coordinates
% External field
quiver3(0,0,0,H(1),H(2),H(3),'y','LineWidth',3,'AutoScaleFactor'
,10);
quiver3(0,0,0,m(1,1),m(1,2),m(1,3),'g','LineWidth',3,'AutoScale',
'off'); %starting magnetization
lgd = legend();
lgd.Position = [0.74 0.74 0.2 0.2];
for j=d:d:new_length

```

```

quiver3(0,0,0,m(j,1),m(j,2),m(j,3), 'k','LineWidth',0.3,'
    AutoScale','off');

legend("$H_{\{a\}}$","$M_{in}$",strcat("t = ",num2str(t(j),4)," ns")
);

legend("Interpreter","latex");

drawnow; %pause(0.05);

end

hold on;

quiver3(0,0,0,m(new_length,1),m(new_length,2),m(new_length,3), 'r',
'LineWidth',3,'AutoScale','off','DisplayName','$M_{fin}$'); %

end magnetization

line(m(:,1),m(:,2),m(:,3),'DisplayName','Trajectory'); %trajectory
%legend("$H_{\{a\}}$","$M_{in}$",strcat("t = ",num2str(t(j),4)," ns")
,'$H_{fin}$','Traiettoria',Interpreter='LaTex');

legend

end

```

Listing A.4: plot\_trajectory.m Draw magnetization vector in 3D

```

function [] = plot_xy(m,Dd,titlename) % Stereographic projection
f = figure(); hold on; grid on;
f.Position = [70 150 900 800]; % Window size
set(gca, 'XAxisLocation', 'origin', 'YAxisLocation', 'origin','
FontSize',18);
title('Magnetization in stereographic plane\ '+titlename,"
Interpreter","latex");
axis(1.6*[-1 1 -1 1]);
axis equal;
plot(m(:,1)./(1+m(:,3)),m(:,2)./(1+m(:,3))); %Plot stereographic
plane mx/(1+mz) ed my/(1+mz)
xlabel('$w_1$', 'Interpreter', 'Latex');
ylabel('$w_2$', 'Interpreter', 'Latex');
end

```

Listing A.5: plot\_xy.m Plot magnetization in xy plane and stereographic plane

```

function [] = plot_gmr(m,t,p,~,i_A,titlename)
f = figure();
f.Position = [70 250 900 800]; % Window size
% Variazione di magnetoresistenza
R0 = 3e3;
deltaR = 1e3;
R = deltaR*dot(m,p'.*ones(length(m),3),2); % Dot product
plot(t,(R0-R)*i_A);
set(gca,'FontSize',18);
title(titlename,"Interpreter","latex");
grid on;
ylabel('GMR voltage [V]')
xlabel('time [ns]');
f = figure();
f.Position = [70 250 900 800];
ind = 20000; % Number of samples
t_sam = linspace(t(end-ind),t(end),ind); % Sampling time
% Interpolating the voltage with more samples
GMR_voltage = interp1(t(end-ind:end),(R0-R(end-ind:end))*i_A,t_sam);
power = GMR_voltage*i_A;
% Average emitted power
P_avg = 1/(t_sam(end)-t_sam(1))*trapz(t_sam,power); % Mean
integral
y = fft(GMR_voltage); % FFT calculation
freq = (0:length(y)-1)/(t(end)-t(end-ind)); % Frequency vector
semilogy(freq,abs(y/ind),'LineWidth',2); % Spectral amplitude
set(gca,'FontSize',18);
grid on;
xlim([0 20]);
% RMS value of GMR voltage
V_RMS = sqrt(trapz(t_sam,GMR_voltage.^2)/(t(end)-t(end-ind)));
% RMS value of harmonic voltage
V_RMS_AC = sqrt(2*trapz((1:length(y)/2-1),abs(y(2:ind/2)/ind).^2));
N_harm = find(islocalmax(abs(y/ind)));
f_harm = freq(N_harm(1:10));

```

```

V_DC = abs(y(1)/ind);
V_harm = 2*abs(y(N_harm(1:10))/ind);
THD = sqrt(sum(V_harm([2,6]).^2))/V_harm(1);
hold on;
text(0,1.0*V_DC,['V_0=',num2str(V_DC,4),' V'],'fontsize',14);
text(f_harm(1),1.1*V_harm(1),['V_1=',num2str(V_harm(1),4),' V'],'
    fontsize',14);
text(f_harm(2),1.1*V_harm(2),['V_2=',num2str(V_harm(2),4),' V'],'
    fontsize',14);
text(f_harm(6),1.1*V_harm(6),['V_3=',num2str(V_harm(6),4),' V'],'
    fontsize',14);
title(['Average absorbed power in last ',num2str(t(end)-t(end-ind)
    ,3),' ns, P_{avg} = ',num2str(P_avg/1e-6,4),' \mu W']);
xlabel('Frequency [GHz]');
ylabel('Voltage spectrum');
end

```

Listing A.6: plot\_gmr.m Gmr calculation



Figure A.1: Scan this code with your smartphone to see the magnetization vector switch from an equilibrium state to the other, under the effect of the spin transfer torque, on the same page it is also possible to download this thesis.

